A Thermo chemical Study of Arcjet Thruster Flow Field

J.-R. Shin, S. Oh, and J.-Y. Choi
Department of Aerospace Engineering
Pusan National University, Busan, 609-735, Korea
tazo@pusan.ac.kr

Keywords: Propulsion, Arcjet, Hydrazine, Chemical Reaction, thermal Radiation

Abstract

Computational fluid dynamics analysis was carried out for thermo-chemical flow field in Arcjet thruster with mono-propellant Hydrazine (N_2H_4) as a working fluid. The theoretical formulation is based on the Reynolds Averaged Navier-Stokes equations for compressible flows with thermal radiation. The electric potential field governed by Maxwell equation is loosely coupled with the fluid dynamics equations through the Ohm heating and Lorentz force. Chemical reactions were assumed being infinitely fast due to the high temperature field inside the arcjet thruster. An equilibrium chemistry module for nitrogen-hydrogen mixture and a thermal radiation module for optically thin media were incorporated with the fluid dynamics code. Thermo-physical process inside the arcjet thruster was understood from the flow field results and the performance prediction shows that the thrust force is increased by amount of 3 times with 0.6KW arc heating.

Introduction

The arcjet thruster is used for orbit transfer or attitude control of a satellite, and also will be used as space propulsion system. The arc heating makes the propellant accelerate to have increased thrust force. The complex characteristics of the flow field consist of high Mach number (4~5), high temperature (5,000~7,000 K), chemically reacting and electrically induced flow. Thus for the analysis of the arcjet flow, the numerical scheme has to handle the high speed flow, electrical effects, radiation effects, turbulent model, and chemical reaction of the propellant. In this study, a conceptual arcjet thruster shown in Fig. 1 is considered with hydrazine (N_2H_4) as a monopropellant. The hydrazine is widely used in small scale thrusters for its good properties as a mono-propellant. Due to the high temperature field inside the arcjet thruster chemical reactions were assumed being infinitely fast with detailed thermo-chemical properties of the chemical components.

Reynolds averaged Navier-Stokes equations were solved simultaneously with the Maxwell equation to consider the effects of electric field. The electric is loosely coupled with the fluid dynamics equations through the Ohm heating term, an arc heat source. Lorentz force was also considered from the electric field as an external force in momentum conservation equation. For the radiation model, Rosseland model has been adopted with the assumption of thick optical thickness of the Hydrazine gas. Turbulence closure was simply made by Baldwin-Lomax algebraic turbulence model. The governing equations were solved by a finite volume fully-implicit TVD(Total Variation Diminishing) code which uses Roe's approximate Riemann solver and MUSCL(Monotone Upstream-centered Schemes for Conservation Laws) scheme. LU-SGS (Lower Upper Symmetric Gauss Seidel) method is used for the implicit solution strategy. The Ohm heating and the Lorentz force were evaluated by at each iteration steps from the solution of the Maxwell equation, an elliptic partial differential equation.

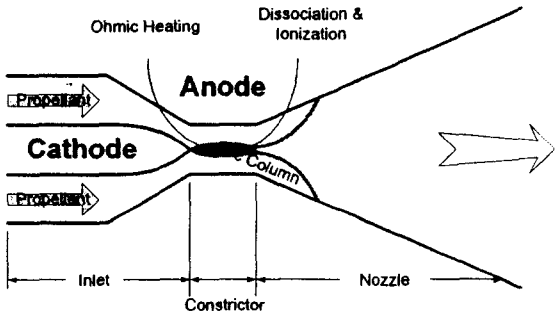

Fig. 1. Conceptual diagram of arcjet thruster and flow field

Theoretical Formulations

Governing Equations

For the simulation of above arcjet thruster, Reynolds Averaged Navier-Stokes equations and formation of thermal plasma by arc discharge employed to analyze the electric chemical equilibrium supersonic viscous flow in axi-symmetric coordinates. The conservation form of these governing equations set is written in curvilinear coordinates as follows.

$$\frac{\partial \mathbf{Q}}{\partial t}+\frac{\partial \bar{\mathbf{F}}}{\partial x}+\frac{\partial \bar{\mathbf{G}}}{\partial r}+\alpha \mathbf{H}=\frac{\partial \bar{\mathbf{F}}_v}{\partial x}+\frac{\partial \bar{\mathbf{G}}_v}{\partial r}+\alpha \mathbf{H}_v+\mathbf{W}$$

$$\mathbf{Q}=[\rho, \rho u, \rho v, e]^T,\ \mathbf{W}=[0,\ F_x,\ F_y, S_{ohm}]^T$$

where F_x, F_y represents the Lorentz forces exerted by the electric field and S_{ohm} is the amount of heat by electric arc. The specific heat of each species is obtained by NASA polynomial data that are valid till to 20,000k

For the turbulent effects, the zero-equation of the Baldwin-Lomax models is used. There are two regions, inner (close to surface) and outer region as

Inner region, $\mu_T = \rho l^2 |\xi|$,

Outer region, $\mu_T = 0.0168 \rho V_0 L_0$

The Prandtl number is assumed as 0.9.

Computational Fluid Dynamics Algorithms

The finite volume cell-vertex scheme is used for spatial discretization of the governing equations. The viscous terms are expressed by a central difference method and the convective terms are expressed as the differences of numerical fluxes at cell interfaces.

$$\left(\frac{\partial \mathbf{Q}}{\partial t}\right)_{i,j} = \mathbf{RES}_{i,j}$$

$$\mathbf{RES}_{i,j} = -J_{i,j}\left(\tilde{\mathbf{F}}_{i+1/2,j} - \tilde{\mathbf{F}}_{i-1/2,j} + \tilde{\mathbf{G}}_{i,j+1/2} - \tilde{\mathbf{G}}_{i,j-1/2}\right) - \mathbf{H}_{i,j}$$

$$+\mathbf{W}_{i,j} + \frac{J_{i,j}}{2}\left(\mathbf{F}_{v\,i+1,j} - \mathbf{F}_{v\,i-1,j} + \mathbf{G}_{v\,i,j+1} - \mathbf{G}_{v\,i,j-1}\right) + \mathbf{H}_{v\,i,j}$$

The numerical fluxes containing artificial dissipation are formulated using Roe's FDS(Flux Difference Splitting) method.

$$\tilde{\mathbf{F}}_{i+1/2,j} = \frac{1}{2}\left[\mathbf{F}(\mathbf{Q}_R) + \mathbf{F}(\mathbf{Q}_L) - \left|\mathbf{A}(\mathbf{Q}_R, \mathbf{Q}_L)\right|(\mathbf{Q}_R - \mathbf{Q}_L)\right]$$

where subscript L and R are the extrapolated values at the left and right grid point of the cell interface (i+1/2). $A(Q_R,Q_L)$ implies that the Jacobian matrix of flux vector F is evaluated by Roe's average of Q_R,Q_L.

MUSCL scheme is used for the extrapolation of primitive variables at the cell interface. The minmod limiter function is used to overcome severe dispersion errors introduced by the high-order extrapolation and to preserve TVD property.

Fully implicit time integration method is used for analysis of supersonic reacting flow. By applying LU-SGS(Lower Upper-Symmetric Gauss Seidal) method which is proposed by Shuen and Yoon. In the LU-SGS method, the governing equations can be integrated fully implicitly by the diagonal lower and upper steps with an approximate Jacobian splitting method.

$$\left[\frac{\mathbf{I}}{\Delta t} + J_{i,j}\left\{\Lambda(\lambda_A) + \Lambda(\lambda_B)\right\} - \mathbf{Z}\right]_{i,j} \Delta\mathbf{Q}^*_{i,j}$$

$$= \mathbf{RES}_{i,j} + J_{i,j}\left(\mathbf{A}^+_{i-1,j}\Delta\mathbf{Q}^*_{i-1,j} + \mathbf{B}^+_{i,j-1}\Delta\mathbf{Q}^*_{i,j-1}\right)$$

$$\left[\frac{\mathbf{I}}{\Delta t} + J_{i,j}\left\{\Lambda(\lambda_A) + \Lambda(\lambda_B)\right\}\right]_{i,j} \left(\Delta\mathbf{Q}^n_{i,j} - \Delta\mathbf{Q}^*_{i,j}\right)$$

$$= -J_{i,j}\left(\mathbf{A}^-_{i+1,j}\Delta\mathbf{Q}^n_{i+1,j} + \mathbf{B}^-_{i,j+1}\Delta\mathbf{Q}^n_{i,j+1}\right)$$

Because the jacobian of chemical source term is considered to be a lower part for computational convenience, full matrix inversion is needed at the lower part. However, only algebraic calculation is needed at the upper part.

The numerical algorithm used in this study is validated with a number of the numerical simulation for the cases where experimental data exist, such as the shock-induced combustion phenomena around a blunt body and the shock/boundary interaction problems.

Arc modeling

The arc electric field can be represented by the Maxwell equation. With the electric-conductivity, which is the function of temperature and pressure of the working fluid,

$$\sigma = \sigma(T, P)$$

The Maxwell equation can be written as

$$\frac{\partial}{\partial x}\left(\sigma\frac{\partial \Phi}{\partial x}\right) + \frac{1}{y}\frac{\partial}{\partial y}\left(\sigma\frac{\partial \Phi}{\partial y}\right) = 0$$

The amount of Ohmic heating can be calculated as.

$$S_{ohm} = \sigma\left(\vec{E}\cdot\vec{E}\right) = \sigma\left|\vec{E}\right|^2$$

where $\vec{E} = -V\ \nabla\Phi$.

Chemistry Modeling

For the current study, the Hydrazine is used as a propellant. The reaction components of the Hydrazine gas are considered as the 4 components of N, N_2, H and H_2. The equilibrium constants of each component are calculated for the temperature. The thermodynamics data for the Hydrazine gas was obtained using NASA polynomial Fit.

The reaction formulation of the Hydrazine gas is

$$N_2H_4 \rightarrow n_1N_2 + n_2N + n_3H_2 + n_4H$$

where

$$\sum_{k=1}^{NS} n_k = 1,\quad R_{H/N} = 2$$

The remaining 5 equations are following reaction equations as,

$$N_2 \leftrightarrow 2N,\ H_2 \leftrightarrow 2H,$$

$$\prod_{k=1}^{NS} n_k^{(\nu''_{r,k} - \nu'_{r,k})} = K_p^r(T)\cdot p^{-\Delta\sum_{k=1}^{NS}(\nu''_{r,k} - \nu'_{r,k})} \qquad r = 1,2$$

Thermal Radiation

The Rosseland approximation is considered, since the working fluid has high temperature from ohmic heating inside the nozzle. Assuming the optically thickness inside the nozzle, the Rosseland model for the heat flux can be written as

$$q_r = -\frac{16}{3}\sigma_{sb}T^3\frac{1}{\alpha_R}\frac{\partial T}{\partial x_i}$$

Inside the gas, the heat fluxes for the conduction and the radiation can be represented as

$$q = q_r + q_c = -\left(\frac{16\sigma_{sb}T^3}{3a_R} + k_c\right)\nabla T$$

With the assumption of thick optical thickness, the ratio between the conductivities of conduction and radiation is

$$\frac{k_c}{k_r} = \frac{k_c}{16\sigma_{sb}T^3/3a_R} = \frac{3k_c a_R}{4\sigma_{sb}T^3} = \frac{3}{4}N$$

Then the heat flux can be simplified as

$$q = q_r + q_c = -\left(\frac{4}{3N}+1\right)k_c \nabla T$$

where N is the radiation-conduction parameter, and for the case of $N < 0.1$, the radiation is dominant.

Computational Result

Configuration and Operating Conditions

The arcjet grid configured 80×40 such as Fig.2 that clustered in cathode tip, nozzle throat and wall. Radius direction of grid is always normal to the axis of symmetry for the evaluation of the arcjet performance.

Fig. 2 The arcjet grid system

For the inflow condition from the thrust chamber, the adiabatic temperature of hydrazine decomposition is calculated and compared in Table 1 with the results from NASA CEA code. Two results show small differences within acceptable range, due to the difference of thermo-chemical data used in both codes.

Components	Present	NASA (CEA2)
N_2	3.3333-01	3.3333-01
N	1.6929-14	6.0190-15
H_2	6.6665-01	6.6666-01
H	1.9968-05	6.6720-06
Temperature	1425.90K	1430.13K
Pressure	0.08Mpa	0.08Mpa

Table. 1 Computing result in chamber

No-slip and adiabatic conditions were used for nozzle boundary and inflow velocity is extrapolated at inlet with all other variables fixed. At nozzle exit, constant low-pressure is applied first, for the fast convergence, and then supersonic out flow condition is applied, if exit Mach number exceed 1.0.

Comparison of Flow Fields

Figure 3 and 4 shows the temperature and Mach number distribution for frozen and equilibrium analysis. Electric potential contours over the temperature distribution and pressure contours over the Mach number distribution are also plotted. Since the Ohm heating is proportional to the gradient of electric potential most of the heat is generated around the axis of symmetry resulting high temperature over there. It is understood from the result that overall temperature of equilibrium analysis is lower than that of frozen flow analysis since the dissociation effect is included in the equilibrium analysis. Figure 5 and 6 shows Radial temperature distribution and Mole fraction distribution at nozzle exit for the equilibrium analysis. This results imply that the average molecular weight is small, the specific heat ratio is high, and the speed of sound is large around the axis of symmetry where the region of strong dissociation. Thus the Mach number distribution around the axis of symmetry shows lower levels in Fig. 4 due to the strong dissociation. The difference between the exit temperatures of frozen and equilibrium analysis is more than 500K, that also results in reduced exit flow speed.

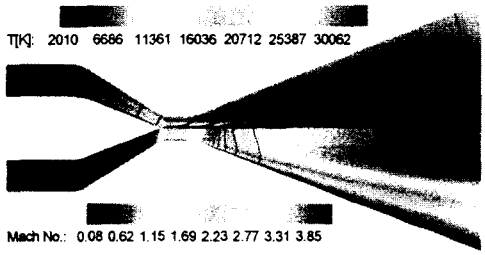

Fig. 3 Temperature and Mach number distribution of frozen flow analysis overlaid with iso-electric potential curves and iso-pressure contours.

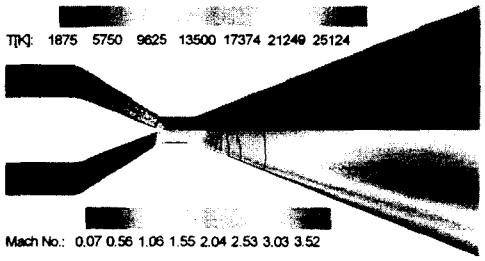

Fig. 4 Temperature and Mach number distribution of equilibrium flow analysis overlaid with iso-electric potential curves and iso-pressure contours.

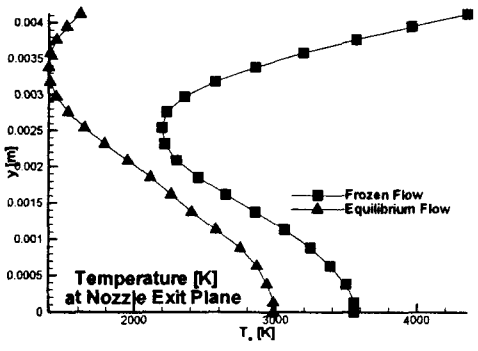

Fig. 5 Radial temperature distribution at nozzle exit.

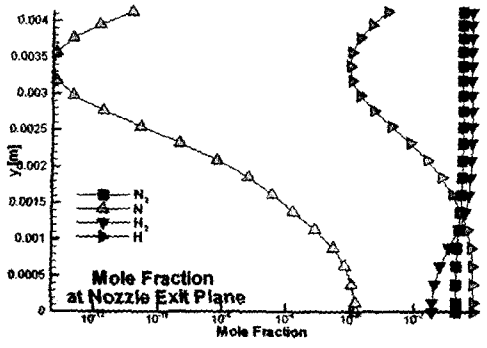

Fig. 6 Mole fraction distribution at nozzle exit.

Performance of Arcjet Thruster

Figure 5 and 6 shows the variations of Mach number and specific impulse along the centerline with respect to the throat to cross section area ratio. For both the frozen and equilibrium analysis it is under stood that the Mach is increasing slowly at large area ratio and specific impulse is nearly unchanged after the area ration of around 30. The specific impulse from the frozen flow analysis 580 s and that from equilibrium analysis is 440 s. So, it is also under stood that the dissociation effect results in about 24% loss of performance based on that the frozen flow analysis.

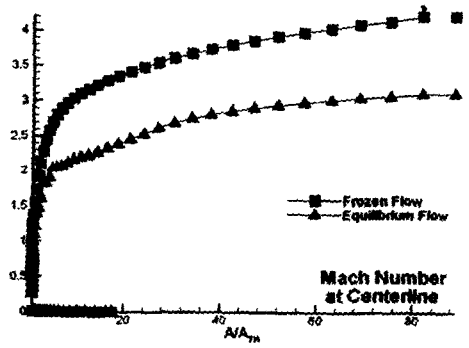

Fig. 7 Mach number variation along the centerline.

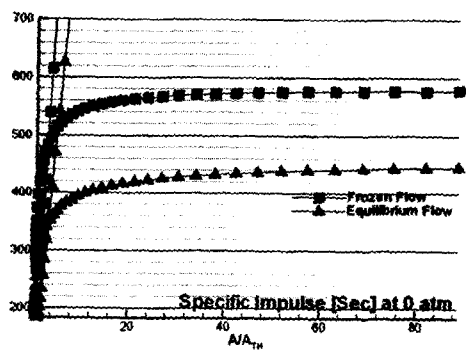

Fig. 8 Variation of specific impulse along the centerline.

Conclusions

The efficient numerical scheme has been developed to analyze the arcjet thruster flow field. The scheme includes the analysis of Reynolds averaged Navier-Stokes equations (Roe's FDM and MUSCL method), the electric arc (Maxwell equation), equilibrium chemical reaction, thermal radiation (Rosseland approximation) and turbulent effect (Baldwin-Lomax model). Through the Maxwell equation, the effects of the Lorentz forces and Ohmic heating are considered, too. The comparison of the frozen and equilibrium flow analysis results in the 24% of performance loss by the chemical dissociation, that would be the maximum value in the view point of chemical kinetic analysis since the frozen and equilibrium results means the zero and complete dissociation from no-reaction and infinitely fast reaction limits.

References

1) Shigeru Kuchi-ishi and Mishio Nishida, "Numerical Simulation of a Nitrogen Arcjet Thruster, Space Transportation", *ISAS January* 13-14, (1999).
2) Kim, C.S., "Navier-Stokes calculation of electric-Arc flow field", Master Thesis, Pusan National University, (1999)
3) KERC Report, "Development of Numerical scheme for the Flow Field around the Circuit Breaker Including Electric Arc", Korea Electric Reserch Center, (1999).
4) Li X. and Wang Q., "Numerical Analysis of Flow Field and the Dynamic Properies of Arc in the Interrupting Chamber of an SF_6 Puffer Circuit Breaker," *IEEE Transection of Plasma Science*, Vol. 25 No. 5, Oct (1997)., pp.962-985.
5) Zhang X.D., Trepanier J.Y., and Camarero R., "Numerical Simulation of a 2kA Convection-Staboilized Nitrogen Arc using FCD Tools," *J. Phys. D: Appl. Phys.* Vol. 30, (1997), pp.3240-3252.
6) Choi, J.-Y., Jeung, I.-S. and Yoon, Y., "Computational Fluid Dynamics Algorithms for Unsteady Shock-Induced Combustion Part 1: Validational Study," *AIAA Journal*, Vol. 38 No 5, May (2000).
7) Park K.Y. and Fang M.T.C., "Mathematical modeling of SF_6 puffer circuit breakers I: high current region",*IEEE Trans. Plasma Sci.* ,vol 24, (1996), pp.490-502.
8) Masaaki S., Yoshihumi S, and Hiroshi A., "Numerical Analysis of the Behavior of Hydrogen Added into a Free Burning Arc", *Plasma chemistry and Plasma processing*, Vol.16. 4, (1996), pp.399-415.
9) Fujiwara T., Fukui T. and Yonezawa F., "A Mode of Laser Propulsion-Axisymmetric Laser-

Supported Detonation," *AIAA Paper* 94-0052, (1994).
10) Hoffmann K.A., "Computational Fluid Dynamics for Engineers, Part 1," Engineering Education System, (1993).
11) Ishikawa M., Suzuki K., and Ikeda H., "Computer simulation of phenomena associated with hot gas in puffer-type gas circuit breaker."*IEEE Trans. Parallel Distrib.*,vol. 6, (1991), pp.833-839.
12) Kuci-ishi, S. and Nishida M. "Numerical Simulation of a Nonequilibrium Plasma Flow in a Nitrogen Arcjet Thruster Using a Three-Temperature Kinetic Model, *Proc. 25th Int. Electric Propulsion Conf.* 1997.
13) Park, C. " Validation of Multitemperature Nozzle Flow Code" *J. Thermophys. Heat Trans.*, (1995), pp9-16 .